



TITLE:

Formation of silver nanoparticles under anodic surface of tellurite glass via thermal poling-assisted ion implantation across solid-solid interface

AUTHOR(S):

Murai, S; Fujita, K; Kawase, S; Ukon, S; Tanaka, K

CITATION:

Murai, S ...[et al]. Formation of silver nanoparticles under anodic surface of tellurite glass via thermal poling-assisted ion implantation across solid-solid interface. JOURNAL OF APPLIED PHYSICS 2007, 102(7): 073515.

ISSUE DATE:

2007-10-01

URL:

<http://hdl.handle.net/2433/50555>

RIGHT:

Copyright 2007 American Institute of Physics. This article may be downloaded for personal use only. Any other use requires prior permission of the author and the American Institute of Physics.

Formation of silver nanoparticles under anodic surface of tellurite glass via thermal poling-assisted ion implantation across solid-solid interface

Shunsuke Murai^{a)}

Department of Material Chemistry, Graduate School of Engineering, Kyoto University, Katsura, Nishikyo-ku, Kyoto 615-8510, Japan

Koji Fujita

Department of Material Chemistry, Graduate School of Engineering, Kyoto University, Katsura, Nishikyo-ku, Kyoto 615-8510, Japan and PRESTO, Japan Science and Technology Agency (JST), 4-1-8, Honcho Kawaguchi, Saitama 332-0012, Japan

Sonoko Kawase, Sakiko Ukon, and Katsuhisa Tanaka

Department of Material Chemistry, Graduate School of Engineering, Kyoto University, Katsura, Nishikyo-ku, Kyoto 615-8510, Japan

(Received 20 June 2007; accepted 11 July 2007; published online 10 October 2007)

We have developed a technique by which poling and ion implantation in solid state are simultaneously accomplished. The technique has been applied to $2\text{Ag}_2\text{O} \cdot 3\text{Na}_2\text{O} \cdot 25\text{ZnO} \cdot 70\text{TeO}_2$ (in mol %) glass. The glass is sandwiched by two cover glasses containing Na^+ and then the thermal poling is carried out. We have accidentally found that Ag nanoparticles are selectively precipitated in the vicinity of the anode-side glass surface. X-ray photoelectron spectroscopy reveals that the glass composition of the anode-side glass surface becomes rich in Na^+ after the thermal poling, which is caused by the Na^+ implantation from the cover glass at the anode side. © 2007 American Institute of Physics. [DOI: [10.1063/1.2770829](https://doi.org/10.1063/1.2770829)]

I. INTRODUCTION

Thermal poling is known as an effective method to induce optical second-order nonlinearity in glasses.^{1–12} The process involves application of a direct current (dc) voltage while heating a glass to temperatures typically at around 300 °C and subsequent cooling of the glass under the application of voltage. It has been argued that the migration of mobile charged ions during the thermal poling causes the formation of an internal electrostatic field, which contributes to the second-order nonlinearity. In most thermal poling experiments, a thin charge depletion layer is created near the anode-side surface since the mobile charged ions are often cations such as Na^+ .

In addition to the second-order optical nonlinearity, the thermal poling process can bring about interesting phenomena into glasses. Recently, bleaching of color assisted by thermal poling was reported for a silicate glass containing Ag nanoparticles.^{13,14} With an application of a dc electric field, Ag nanoparticles in the vicinity of the anode-side glass surface are selectively oxidized to Ag^+ , converting a region under the electrode from dark green to transparent. The mechanism of bleaching can be interpreted in terms of electromigration or electrolysis of Ag metal in the vicinity of anode and subsequent migration of Ag^+ .¹⁵ due to the intense electric field in the depletion layer underneath the anode, Ag particles release electrons to become Ag^+ .

In this study, we add one phenomenon to the list of

poling-induced effects. We have performed the thermal poling for a tellurite glass containing Ag^+ and found that Ag nanoparticles are selectively precipitated in the vicinity of the anode-side glass surface. Although this phenomenon appears similar to the earlier-mentioned poling-assisted bleaching in the respect that the reaction relevant to Ag occurs beneath the anode-side glass surface, the physical background is very different: Ag^+ is reduced to Ag metal in the present case, whereas Ag metal is oxidized to Ag^+ in the previous report. It is surprising that reduction takes place at the anode side, where oxidation is usually observed. In the present thermal poling process, alkali-containing cover glasses are placed between the tellurite glass sample and electrodes to avoid an undesired discharge between the electrodes. The presence of alkali-containing cover glasses is found to play an important role in the precipitation of Ag: Na^+ in the cover glass is implanted into the anodic surface of the tellurite glass sample during the thermal poling. The phenomenon observed is analogous to the ion implantations via gas or liquid phases, where charged species are introduced to a solid without valence modifications, and could be referred to as “poling-assisted ion implantation.”

II. EXPERIMENTAL PROCEDURE

Glass with a composition of $2\text{Ag}_2\text{O} \cdot 3\text{Na}_2\text{O} \cdot 25\text{ZnO} \cdot 70\text{TeO}_2$ (in mol %) was prepared by conventional melt-quenching method using reagent-grade AgNO_3 (99.8%), Na_2CO_3 (99.5%), ZnO (99.99%), and TeO_2 (99.999%). The resultant glass was annealed at around its glass-transition temperature ($T_g = 297$ °C), cut into a rectangular shape, and

^{a)}Author to whom correspondence should be addressed. FAX: +81-75-383-2420. Electronic mail: murai@dipole7.kuic.kyoto-u.ac.jp

TABLE I. Conditions of poling. The notation reflects a set of cover glasses used and poling time. AC and AF refer to alkali-containing and alkali-free cover glasses, respectively. The compositions of cover glasses are given in the text.

Sample notation	Cover glasses	Poling time (min)
AC15	AC	15
AC60	AC	60
AC120	AC	120
AF60	AF	60

polished to the thickness of 2 mm for optical measurements. The plate-like glass sample was then sandwiched in between two cover glasses of 0.1 μm thick. Two types of cover glasses purchased from Matsunami Glass Ind. Co., Ltd. were used: one containing alkali ions (referred to as AC cover glass, $4.5\text{K}_2\text{O} \cdot 7.7\text{Na}_2\text{O} \cdot 1.3\text{BaO} \cdot 5.8\text{ZnO} \cdot 1.9\text{Al}_2\text{O}_3 \cdot 8.4\text{B}_2\text{O}_3 \cdot 70.4\text{SiO}_2$ in mol %), and the other essentially free of alkali ions (AF cover glass, $0.1\text{Na}_2\text{O} \cdot 11.9\text{BaO} \cdot 9.1\text{Al}_2\text{O}_3 \cdot 14.5\text{B}_2\text{O}_3 \cdot 64.4\text{SiO}_2$ in mol %). The tellurite glass sample sandwiched was physically contacted with electrodes made of stainless steel and heated to 300 °C. After the glass sample was held at 300 °C for 30 min, a dc voltage of 3.0 kV was applied. After a specific poling time, the glass sample was cooled down while maintaining the applied electric field. The voltage was removed at room temperature. The poling conditions are listed in Table I. Each notation in the table reflects the poling time and the kind of cover glasses used. For instance, AC60 means that the sample was poled for 60 min with AC cover glasses on both the anode and cathode sides.

X-ray diffraction (XRD) analysis was carried out with a diffractometer (RINT 2500, Rigaku, Japan) using $\text{Cu } K_\alpha$ radiation and optical absorption was measured with a Jasco-V570 ultraviolet-visible-near infrared spectrophotometer. X-ray photoelectron spectroscopy (XPS) (MT-5500, Ulvac-Phi, Japan) was performed with $\text{Mg } K_\alpha$ radiation to investigate the composition of the glass surface. Before the measurement, the sample was sputtered by Xe^+ with an energy of 3 keV for 1 min to clean the surface. Binding energies were referenced to C 1s level (284.8 eV) of residual graphitic carbon. The glass composition was also measured by energy-dispersive x-ray spectroscopy (EDS) (EnergyMax, Horiba, Japan).

III. RESULTS AND DISCUSSION

A selective coloration is observed on the anode side of the tellurite glass surface when the glass is thermally poled with AC cover glasses (AC15, AC60, and AC120). As a demonstration, a photograph of the sample poled with a small circular AC cover glass on the anodic surface is displayed in Fig. 1(a). The poling time is 60 min and the applied voltage is set to 1.5 kV so as not to discharge from the edge of the cover glass. In the picture, the upper face of the glass corresponds to the anode-side surface. The selective conversion in color under the area in contact with the cover glass is obvious. The color disappears when the anode-side surface of the poled glass is mechanically etched [Fig. 1(b)]. In con-

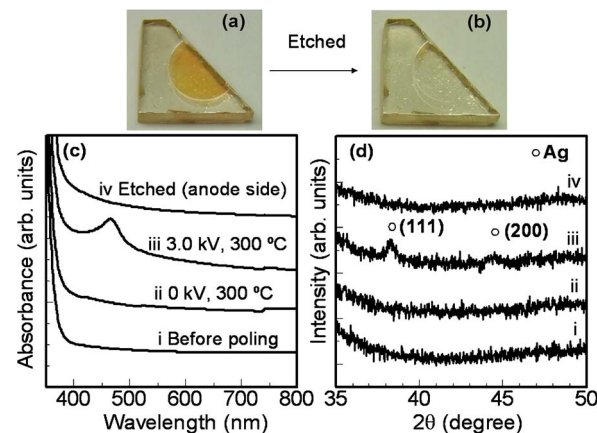


FIG. 1. (Color online) (a) Optical image for the poled glass viewed from the anode-side surface. The poling was performed at 300 °C with a 1.5 kV dc voltage for 60 min. (b) Optical image for the poled glass described in Fig. 1(a) after mechanical etching of the anode-side surface. (c) Optical absorption spectra for $2\text{Ag}_2\text{O} \cdot 3\text{Na}_2\text{O} \cdot 25\text{ZnO} \cdot 70\text{TeO}_2$ glasses: (i) before poling; (ii) after heat treatment at 300 °C without a dc voltage for 60 min; (iii) after poling at 300 °C with a 3.0 kV dc voltage for 60 min (sample AC60); and (iv) after removing 2 μm of the anode-side surface of AC60. (d) XRD patterns for $2\text{Ag}_2\text{O} \cdot 3\text{Na}_2\text{O} \cdot 25\text{ZnO} \cdot 70\text{TeO}_2$ glasses: (i) before poling; (ii) after heat treatment at 300 °C without a dc voltage for 60 min; (iii) anode side of the sample AC60; and (iv) anode side of the sample AC60 after removing 2 μm of the anode-side surface.

trast, no change in color occurs when the thermal poling is performed with AF cover glasses (AF60). In order to examine the origin of coloration, optical absorption spectra and XRD patterns were measured. The results for AC60 are shown in Figs. 1(c) and 1(d) together with those for the glass before poling and the glass heat treated at 300 °C without an electric field. Also shown are the results for AC60 after mechanical etching of 2 μm of the surface. Figure 1(c) exhibits the optical absorption spectra. All four spectra manifest an intense absorption band at wavelengths shorter than 380 nm, which corresponds to the fundamental absorption in the tellurite glass. For AC60, an extinction peak appears at around 470 nm in the spectrum, which is attributable to the surface plasmon resonance of Ag nanoparticles.¹⁶ When the anode-side surface of AC60 is etched, the extinction peak completely disappears as indicated in Fig. 1(b), confirming that the precipitation occurs beneath the anode-side surface only. The variation in XRD pattern [Fig. 1(d)] can be interpreted in a way consistent with the results of optical absorption. The XRD pattern for the anode-side surface of AC60 confirms the precipitation of Ag: diffraction peaks are observed at $2\theta=38^\circ$ and 44° , which are indexed to (111) and (200) planes of cubic Ag phase, respectively. The diffraction peaks completely vanish after the removal of the anode-side surface of AC60.

Figure 2(a) shows the differences in absorbance between before-poling state and poled glasses with different poling times (AC15, AC60, and AC120). With an increment of the poling time from 15 to 120 min, a monotonic increase is observed in the intensity of absorption peak. The radius and volume fraction of Ag particles were evaluated by the Mie scattering theory¹⁷ combined with the Drude free-electron theory.¹⁸ According to the Mie theory, the absorption coefficient α for a medium with a refractive index of n , in which

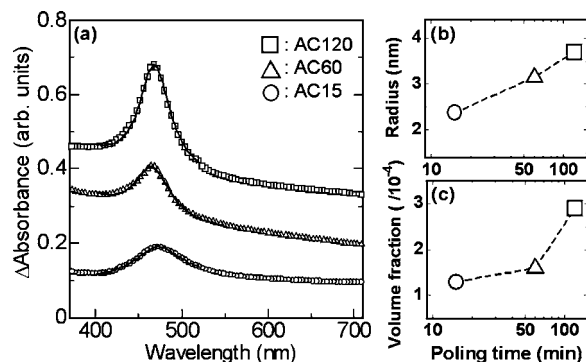


FIG. 2. (a) A difference in absorbance between before and after poling for $2\text{Ag}_2\text{O} \cdot 3\text{Na}_2\text{O} \cdot 25\text{ZnO} \cdot 70\text{TeO}_2$ glasses with a poling time of 15 min (open circles), 60 min (open triangles), and 120 min (open squares). Solid curves are calculated ones based on the Mie scattering theory. (b) Mean particle size, R , of the Ag particles as a function of poling time. (c) Volume fraction, Q , of the Ag particles. Both R and Q were estimated from the theoretical fits.

spherical metal nanoparticles much smaller than the wavelength of incident light are dispersed, is given by¹⁹

$$\alpha = \frac{9Qn^3\omega}{c} \frac{\varepsilon_2}{(\varepsilon_1 + 2n^2)^2 + \varepsilon_2^2}, \quad (1)$$

where ω and c are the angular frequency and the speed of light, respectively; Q is the volume fraction of nanoparticles; and ε_1 and ε_2 are the real and imaginary parts of the dielectric function of the metal, ε , i.e., $\varepsilon = \varepsilon_1 + i\varepsilon_2$. The dielectric function is modeled by a Drude free-electron equation as $\varepsilon = 1 - \omega_p^2 / (\omega^2 + i\omega\gamma)$, where ω_p is the plasma frequency and γ is the mean collision rate of the conduction electrons. For particles much smaller than the mean free path of electrons in bulk material (~ 30 nm for Ag at room temperature²⁰), γ can be related to the radius of particles R as $\gamma = \gamma_b + Av_f/R$,²¹ where γ_b is the bulk free-electron relaxation frequency and v_f is the Fermi velocity ($v_f = 1.39 \times 10^6$ m/s for Ag).²⁰ A is a geometric factor and is often taken to be unity. Then, the Drude equation is substituted for Eq. (1) with the condition of $\omega \gg \gamma$, which is valid in the range of visible light. The resultant equation is fit to the experimental curves with $n = 2.02$ taken from the literature for $\text{Na}_2\text{O}-\text{ZnO}-\text{TeO}_2$ glass,¹¹ $\hbar\gamma_b = 0.022$ eV calculated from the data in Ref. 22, and R , Q , and ω_p as fitting parameters. The solid curves in Fig. 2(a) represent results of fitting, and R and Q estimated are displayed in Figs. 2(b) and 2(c), respectively. Here, Q was deduced under a rough assumption that the effective thickness of the glass was $2 \mu\text{m}$. Both R and Q monotonically increase as the poling time is increased. The values of $\hbar\omega_p$ take 7.9, 8.0, and 8.0 eV for AC15, AC60, and AC120, respectively, which are comparable to the bulk value calculated from data in Ref. 22, 9.2 eV. Note that the R obtained contains some uncertainty since Eq. (1) includes several assumptions. For the purpose of obtaining the shape and spatial configuration of metal nanoparticles, direct observation using transmission electron microscopy would be effective.

The experimental fact that the Ag precipitates only when the poling is performed with AC cover glasses indicates that some chemical and/or physical reaction is induced by the presence of AC cover glass. In order to elucidate a role of the cover glass, XPS was measured for the anode-side glass sur-

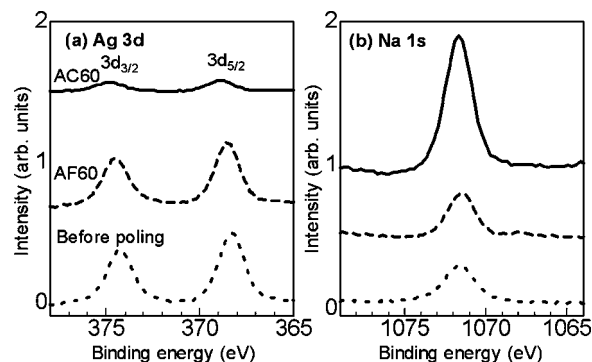


FIG. 3. XPS spectra in regions of Ag 3d (a) and Na 1s (b). The solid, dashed, and dotted curves denote the spectra for the anode side of AC60, anode side of AF60, and the glass before poling, respectively.

faces of AC60, AF60, and the glass before poling. Figure 3(a) shows the photoelectron spectra of Ag 3d. In each spectrum, peaks attributed to Ag $3d_{5/2}$ and $3d_{3/2}$ appear at binding energies of around 368 and 374 eV, respectively. No systematic shift of binding energies is seen. The peak intensity for AC60 is smaller than those for AF60 and the glass before poling, although Fig. 1 confirms that the precipitation of Ag occurs on the anode side of AC60. Taking into account the fact that XPS provides information about a surface, the absence of intense Ag 3d peaks indicates that the Ag particles are not precipitated on the very surface of the tellurite glass, but embedded somewhere within a region of $2 \mu\text{m}$ in depth from the surface. To rule out the possibility that the Ag particles were removed during the Xe^+ sputtering, we measured the spectrum for AC60 before the sputtering, and observed no intense peaks due to Ag. In Fig. 3(b), Na 1s photoelectron spectra are displayed. Similarly to the case of Ag 3d, no systematic shift is seen in binding energies. The peak intensity in the spectrum for AC60 is very strong compared to those for AF60 and the glass before poling, suggesting an increase in Na content. From the EDS measurement, the same results, i.e., a decrease in Ag concentration and an increase in Na concentration, are obtained for the anode-side surface of AC60.

The increase in Na content is caused by the migration of Na^+ from the cover glass.^{10,12} During the poling, relatively mobile cations such as Na^+ drift toward a cathode to screen the applied voltage. As a result of the migration, a cation-depleted layer with a net negative charge is created near the anode-side surface because the anions in the glass, i.e., bridging and nonbridging oxide ions, are more strongly stuck to the glass network and, hence, are immobile. Lack of mobile carriers leads to a high resistivity of the depletion layer, and thus, the voltage tends to drop across the layer instead of the whole bulk. According to a simple calculation which ignores other resistive elements, an application of 3.0 kV can bring about an electric field of an order of 10^8 V/m across a depletion layer typically about $10 \mu\text{m}$ thick. The intense electric field allows Na^+ in the cover glass to penetrate into the tellurite glass so as to compensate for the net negative charge. Consequently, accumulation of Na^+ beneath the anode-side glass surface is attained. Since Na^+ is a typical network modifying cation in glass structure, the glass transi-

tion temperature of the layer rich in Na^+ may become lower than that of the bulk glass. Therefore, the supply of heat at 300 °C causes vigorous viscous flow in the accumulation layer and can possibly facilitate thermal reduction of Ag^+ to Ag.

IV. CONCLUSION

In conclusion, we have conducted the thermal poling for $2\text{Ag}_2\text{O} \cdot 3\text{Na}_2\text{O} \cdot 25\text{ZnO} \cdot 70\text{TeO}_2$ glass sandwiched in between two cover glasses containing Na^+ and found that Ag nanoparticles were selectively precipitated in the vicinity of the anode-side glass surface. An increase in Na^+ concentration due to the migration from the cover glass plays an important role in the precipitation process. The thermal poling-assisted Na^+ doping demonstrated in the present study can be regarded as an ion implantation via the solid-state phase, in analogous to the conventional ion implantations via gas or liquid phases. It is interesting to investigate the detailed mechanism of ion implantation across the solid-solid interface from a point of view of surface modification of glasses. Such a study is in progress.

ACKNOWLEDGMENTS

This study was supported by the Grant-in-Aid for Scientific Research (No. 18360316) and Young Scientist (B) from the Ministry of Education, Culture, Sports, Science, and Technology, Japan. The authors also acknowledge the financial support from Nippon Sheet Glass Foundation for Materials Science and Engineering.

- ¹R. A. Myers, N. Mukherjee, and S. R. J. Brueck, *Opt. Lett.* **16**, 1732 (1991).
- ²A. Okada, K. Ishii, K. Mito, and K. Sasaki, *Appl. Phys. Lett.* **60**, 2853 (1992).
- ³H. Nasu, H. Okamoto, A. Mito, J. Matsuoka, and K. Kamiya, *Jpn. J. Appl. Phys., Part 2* **32**, L406 (1993).
- ⁴K. Tanaka, K. Kashima, K. Hirao, N. Soga, A. Mito, and H. Nasu, *Jpn. J. Appl. Phys., Part 2* **32**, L843 (1993).
- ⁵P. G. Kazansky, L. Dong, and P. St. J. Russell, *Electron. Lett.* **30**, 1345 (1994).
- ⁶K. Tanaka, K. Kashima, K. Hirao, N. Soga, A. Mito, and H. Nasu, *J. Non-Cryst. Solids* **185**, 123 (1995).
- ⁷K. Tanaka, A. Narazaki, K. Hirao, and N. Soga, *J. Non-Cryst. Solids* **203**, 49 (1996).
- ⁸T. Takebe, P. G. Kazansky, and P. S. J. Russell, *Opt. Lett.* **21**, 468 (1996).
- ⁹K. Tanaka, A. Narazaki, K. Hirao, and N. Soga, *J. Appl. Phys.* **79**, 3798 (1996).
- ¹⁰A. Narazaki, K. Tanaka, K. Hirao, and N. Soga, *J. Appl. Phys.* **83**, 3986 (1998).
- ¹¹K. Tanaka, A. Narazaki, and K. Hirao, *Opt. Lett.* **25**, 251 (2000).
- ¹²K. Tanaka, A. Narazaki, Y. Yonezaki, and K. Hirao, *J. Phys.: Condens. Matter* **12**, L513 (2000).
- ¹³O. Deparis, P. G. Kazansky, A. Abdolvand, A. Podlipensky, G. Seifert, and H. Graener, *Appl. Phys. Lett.* **85**, 872 (2004).
- ¹⁴O. Deparis, P. G. Kazansky, A. Podlipensky, A. Abdolvand, G. Seifert, and H. Graener, *Appl. Phys. Lett.* **86**, 261109 (2005).
- ¹⁵T. Dunn, G. Hetherington, and K. H. Jack, *Phys. Chem. Glasses* **6**, 16 (1965).
- ¹⁶U. Kreibig and M. Vollmer, *Optical Properties of Metal Clusters* (Springer, Berlin, 1995).
- ¹⁷G. Mie, *Ann. Phys. (Paris)* **25**, 377 (1908).
- ¹⁸P. Drude, *Ann. Phys.* **1**, 566 (1900).
- ¹⁹G. W. Arnold, *J. Appl. Phys.* **46**, 4466 (1975).
- ²⁰C. Kittel, *Introduction of Solid State Physics*, 7th ed. (Wiley, New York, 1996).
- ²¹U. Kreibig and C. v. Fragstein, *Z. Phys.* **224**, 307 (1969).
- ²²P. B. Johnson and R. W. Christy, *Phys. Rev. B* **6**, 4370 (1972).